OPEN

Iterative Time-Reversed Ultrasonically Encoded Light Focusing in Backscattering Mode

Haowen Ruan[1]*, Mooseok Jang[1]*, Benjamin Judkewitz[1,2] & Changhuei Yang[1]

[1]Electrical Engineering, California Institute of Technology, 1200 E California Boulevard, Pasadena, California, 91125, USA, [2]NeuroCure Cluster of the German Excellence Initiative, Charité Berlin, Charitéplatz. 1, 10117 Berlin, Germany.

The Time-Reversed Ultrasound-Encoded (TRUE) light technique enables noninvasive focusing deep inside scattering media. However, the time-reversal procedure usually has a low signal-to-noise ratio because the intensity of ultrasound-encoded light is intrinsically low. Consequently, the contrast and resolution of TRUE focus is far from ideal, especially in the backscattering geometry, which is more practical in many biomedical applications. To improve the light intensity and resolution of TRUE focus, we developed an iterative TRUE (iTRUE) light focusing technique that employs the TRUE focus itself as a signal source (rather than diffused light) for subsequent TRUE procedures. Importantly, this iTRUE technique enables light focusing in backscattering mode. Here, we demonstrate the concept by focusing light in between scattering layers in a backscattering configuration and show that the light intensity at the focus is progressively enhanced by a factor of ~20. By scanning across a fluorescent bead between these two scattering layers, the focusing resolution in the ultrasound axial and lateral directions was improved ~2-fold and ~3-fold, respectively. We further explored the application of iTRUE in biological samples by focusing light between 1 mm thick chicken tissue and cartilage, and light intensity enhancements of the same order were also observed.

F
ocusing light inside scattering media such as biological tissues is attractive, especially in biomedical applications. However, this is a challenging task because optical scattering must be overcome. The iterative optimisation based technique[1] has been developed to focus light to an area of interest. This technique optimises the spatial light modulator by maximising the feedback signal. Transmission matrix measurement[2] is another technique that enables light focusing through scattering media. Instead of iteratively optimising a wavefront or measuring a transmission matrix, phase conjugation techniques directly obtain the required wavefront at high speed, using nonlinear media[3,4] or imaging sensor arrays via Digital Optical Phase Conjugation (DOPC)[5]. DOPC records the optical wavefront from the target and plays back the phase-conjugated light, which traces back to its origin due to time-reversal symmetry. However, all of these techniques require a 'guide star' or sensors behind or inside the scattering medium. These guide stars could be direct light sources[6,7], photoacoustic based objects[8,9], optical nonlinear particles[10], or an ultrasound focus[11–14]. Among these sources, an ultrasound focus is the best fit for noninvasive operation because it creates a virtual source inside the scattering medium by modulating the frequency of the scattered light.

Time-reversed ultrasound-encoded light was first demonstrated using a photorefractive crystal as a wavefront recording and modulating medium[11]. However, the crystal provided low optical gain and thus had limited potential for applications requiring focusing deep inside highly scattering medium. Although nonlinear polymer films are able to enhance the optical gain[15], the gain is still much lower than that obtained by the DOPC method, which has a theoretically infinite optical gain that is practically limited by the damage threshold of the optics[5]. Using DOPC as a phase conjugation engine for TRUE, deep tissue fluorescence imaging has been demonstrated[12,13]. Moreover, digital TRUE allows for manipulation of the measured phase map and thus provides advantages such as resolution improvement[16].

One of the factors that limits the applications of the TRUE method is the low focusing peak intensity to the background intensity (with uncontrolled light illumination) ratio (peak-to-background ratio; PBR) resulting from the low detected intensity of ultrasound modulated light. In deep tissue imaging applications, for example, only a small proportion of light will travel through the ultrasound focus, which is very tight (typically <100 μm), to obtain a high resolution image. Of the light that is in the focus, only a small proportion will be modulated by

1

ultrasound with an intensity at diagnostic ultrasound levels[17]. Therefore, it is challenging to measure an accurate phase map of the ultrasound modulated light because of the low signal-to-noise ratio (SNR). The low SNR limits the applications of TRUE, such as focusing in backscattering mode that is more practical in biological applications. Although analogue TRUE in reflection mode has been demonstrated[18], it also has the problem of low optical gain, as discussed above.

An intuitive approach to solve the low ultrasound modulation efficiency in TRUE would be using the TRUE technique itself because it can deliver stronger light at the focus of the ultrasound. This method would in return result in a more accurate phase map and, consequently, higher light intensity at the ultrasound focus. By iterating this process, the light intensity at the ultrasound focus would be significantly enhanced. Technically, this requires DOPC to simultaneously record the ultrasound modulated light and play back its amplified phase-conjugated copy. A dual-DOPC-based TRUE setup was proposed for this purpose[19], but the system was redundant and was difficult to fit in the backscattering mode, which is critical in many applications such as biomedical imaging. Very recently, a continuous scanning-based TRUE scheme was demonstrated to be able to enhance light intensity with a single DOPC based setup[20]. This work focused on a novel scanning scheme but did not demonstrate or quantify the light intensity enhancement and resolution improvement capabilities in backscattering mode.

In this paper, we report an iterative time-reversed ultrasound-encoded (iTRUE) light technique that can be used to focus light in backscattering mode. We observed a significant enhancement of the light intensity at the ultrasound focus and resolution improvement in images obtained using this technique. It should be noted that the terms iterative/iteration here refer to the repeating of the ultrasound modulation and phase conjugation process and should not be confused with that used for searching for an optimised wavefront based on feedback signals. The reported iTRUE system simultaneously and iteratively detects the ultrasound modulated light and plays back its amplified phase conjugated copy. This system has an intrinsic capability for operation in backscattering mode and can be easily adapted to the transmission mode. We further demonstrate the advantage of backscattering mode operation by focusing light between biological tissue and cartilage. We also demonstrate the intensity enhancement and resolution improvement in a simulation and discuss the possible mechanisms and limitations of these effects in this paper.

Results

Principle. The working principle of iTRUE is shown in Fig. 1. The setup consists of a DOPC module and an ultrasound modulation module (Fig. 1a). A collimated laser beam (frequency f0) is launched to the phase-only SLM with an arbitrary or blank (Fig. 1b wavefront) phase display. The reflected light, serving as a probe beam, enters the scattering sample and diffuses, as shown in Fig. 1b. As the first step of TRUE (recording), ultrasound modulates the probe beam by shifting its frequency by the ultrasound frequency fus (Fig. 1c). The backscattered ultrasound-modulated light as well as the unmodulated portion travel back to the beam splitter (ii) and then to the camera. In order to selectively measure the phase of the ultrasound-modulated light (Fig. 1c wavefront), a reference beam with a frequency tuned to f0 + fus is used to interfere with the backscattered light, resulting in a static fringe pattern for the modulated light, while the unmodulated portion does not interfere coherently. In this case, a 4-phase stepping method[21] or off-axis holography can be used to record the phase map of the ultrasound-modulated light. In the second step (playback), the recorded wavefront is phase-conjugated (Fig. 1d wavefront) and sent to the SLM. The collimated probe beam is then modulated by the SLM and creates a focus at the ultrasound focus due to the time-

reversal symmetry (Fig. 1d). The first step is then repeated, but this time stronger ultrasound-modulated light is generated (Fig. 1d) due to the results of the previous step. This procedure leads to a more accurate phase map (Fig. 1e wavefront) and, consequently, higher playback light intensity at the focus (Fig. 1e). As can be seen from the iTRUE setup, the iTRUE process requires that playback of the phase-conjugated light and the next recording of the wavefront occur simultaneously.

Simulation. To better understand the steps of the iTRUE process, we carried out a simulation. In this simulation, the performance of the system in terms of noise was shot noise limited. We assumed the average number of ultrasound-modulated photons per pixel is 10^{-2} and that of the unmodulated photons is 100. The average number of photons of the reference beam was 10^4, which is ~100 times higher than the signals (modulated and unmodulated light). These assumptions are based on estimations from a typical hologram captured in our TRUE system. In this simulation, only the shot noise from the reference beam was considered because the reference beam intensity is much higher than the intensity of the modulated and unmodulated photons. Therefore, shot noise from the unmodulated light could be neglected in the simulation. The interference between the modulated light and the reference beam is given by

$$I_i = I_0 + I_{us} + 2\sqrt{I_0 I_{us}} \cos(\phi_0 + \phi_{us}), \qquad (1)$$

where I_0 and I_{us} are the reference beam intensity and the modulated light intensity, respectively, in the units of photons; ϕ_0 and ϕ_{us} are the corresponding phases. The SNR of this interferogram can then be defined as[17]

$$SNR = \frac{2\sqrt{I_0 I_{us}}}{\sqrt{I_0 + I_{us}}} \approx 2\sqrt{I_{us}}. \qquad (2)$$

Plugging in the number of ultrasound modulated photons, we have

$$SNR \approx 0.2. \qquad (3)$$

Although the SNR is very low at the beginning of the iTRUE iterations, light focusing at the focus of ultrasound can still be obtained because DOPC has a high tolerance for phase error[5]. The playback focus then contributes to a higher modulated light intensity while the shot noise level is maintained, thus yielding a higher SNR measurement and a more accurate phase map, which in return creates a stronger focus at the ultrasound focus. Repeating this process in the simulation gave an iterative increase of SNR and a reduction in the phase error (Fig. 2a). As a result, a progressively enhanced light focus over the number of iterations was obtained (Fig. 2b). By fitting a Gaussian function to the scattered field in the virtual ultrasound focus, the full width at half maximum (FWHM) of the light focus was obtained during each iteration (Fig. 2b). A reduction of FWHM was observed during iteration because a Gaussian ultrasound profile was defined in this simulation. In this case, the multiplication of the profile during each iteration results in a narrower width. The error bars shown in Fig. 2 were calculated based on the standard deviation of 10 simulations.

Direct visualisation of the optical focus. In order to demonstrate the intensity and enhancement with iTRUE, we used a quantum dot sheet to visualise the focusing profile of the phase conjugated light between two scattering media. The design of the sample is shown in Fig. 3a. A quantum dot sheet with a thickness of 500 μm was embedded in a block of clear agarose gel. The gel was placed between two scattering media, with a layer of scattering film on the front and a piece of white eggshell on the back. The distance between the two scattering media was ~6 mm. A camera (Stingray F145, Allied vision technologies, Germany) with its imaging plane at the
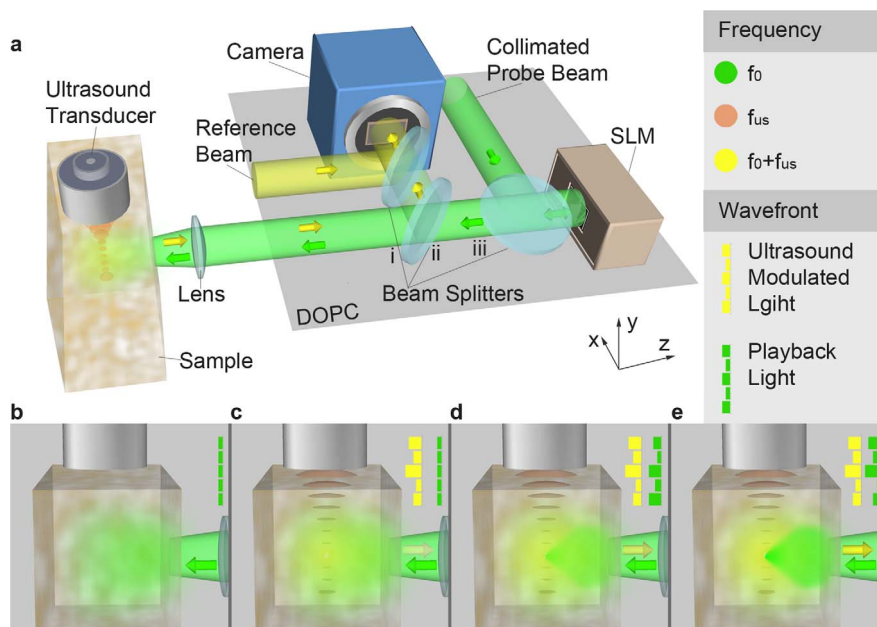
Figure 1 | Principle of iTRUE. (a) Schematic experimental setup consisting of a DOPC system and an ultrasound modulation module. The probe beam reflected off the SLM is scattered by the sample and modulated by the ultrasound. The phase map of the ultrasound modulated light is measured by the camera and the conjugated phase map is displayed on the SLM, which modulates the probe beam again. (b)–(e) Schematic demonstration of signal enhancement with iTRUE. (b) Without ultrasound modulation, the probe beam diffuses inside the scattering sample when the SLM is initially uncontrolled. (c) With ultrasound modulation, a small fraction of the probe beam is shifted in frequency and backscattered to the DOPC system. (d) The phase-conjugated copy of the measured ultrasound-modulated light is sent back to the sample. Although SNR of the measured wavefront is low, owing to the small amount of light being modulated in c, the playback light is still able to create a focus at the focus of the ultrasound. This playback light focus is modulated simultaneously by the ultrasound, and a more accurate wavefront can be measured for the next step. (e) A stronger light focus can thus be obtained. By repeating the playback and recording process, the light intensity focused at the focus of the ultrasound can be progressively increased.

focus of the ultrasound transducer was used to image the light emission light profile from the quantum dot sheet. Without TRUE, the probe beam was scattered by the scattering film and the eggshell, resulting in a diffused background (Fig. 3b). By implementing TRUE, a weak light focus can be observed, as shown in Fig. 3c. The light focus here was much weaker than what has been demonstrated in transmission mode[12,13] because the detected ultrasound-modulated light in backscattering mode is much weaker. By implementing iTRUE, significant light intensity enhancement was observed on the fluorescent quantum dot sheet, as shown in Fig. 3d–f, in which 2, 4 and 8 iterations were performed, respectively. To further enhance the contrast of the light foci, background subtraction[12] was implemented for each image of the light focus. In this case, the background for each image was measured when the conjugated phase map on the SLM was shifted by 50 x 50 pixels during each

iteration. Corresponding images with background subtraction are shown in Fig. 3g–j.

To quantify the intensity enhancement with iTRUE, we analysed the emission light intensity at the ultrasound focal zone. In this case, an area of interest with 200 pixels (323 μm) in the y direction and 50 pixels (81 μm) in the z direction was applied to the area, as shown in between the colour blocks of Fig. 3g–j. One-dimensional images were then taken by averaging these areas of interest in the z direction, as shown in Fig. 3k, in which significant light intensity enhancement can be observed. A Gaussian profile was fitted to each of these one-dimensional images, as shown in Fig. 3k. Taking the peak of each fitted Gaussian profile for the one-dimensional images from the first 8 iTRUE iterations, the intensity enhancement factor (the ratio between the peak intensity at each iteration to that at the first TRUE light focus) was quantified (Fig. 3l). For comparison, the intensity enhancement factor calculated based on the ultrasound-modulated light intensity detected by the DOPC system using digital holography is also shown in Fig. 3l. The intensity enhancement factor at the ultrasound focus after 8 iterations was ~22 based on the fluorescent signals and ~32 based on the holography measurement.

Theoretically, the light intensity enhancement factor measured based on fluorescent signals and holography should be identical. However, the difference in the light intensity enhancement factors can be observed in Fig. 3l. One of the possible reasons for the inaccuracy could be the low light intensity at the first TRUE light focus compared with the considerable background. The other possible reason could be the nonlinearity of the two approaches. Light intensity oscillation can also be observed in Fig. 3l. One explanation for this oscillation is that the size of the ultrasound focus is much larger than that of an optical speckle. In this case, two sets of optical modes can oscillate during the iTRUE process. Another possible reason is that light travels through different channels of the scattering sample before and after ultrasound modulation during one iteration. To
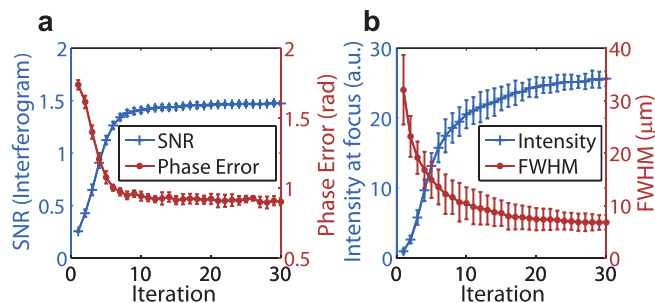

Figure 2 | Simulation results of the iTRUE process. (a) SNR of the interferogram and the phase error (mean absolute) at the imaging sensor plane over the sequence of iterations. (b) Intensity enhancement and resolution improvement at the focus of the ultrasound over the sequence of iterations.
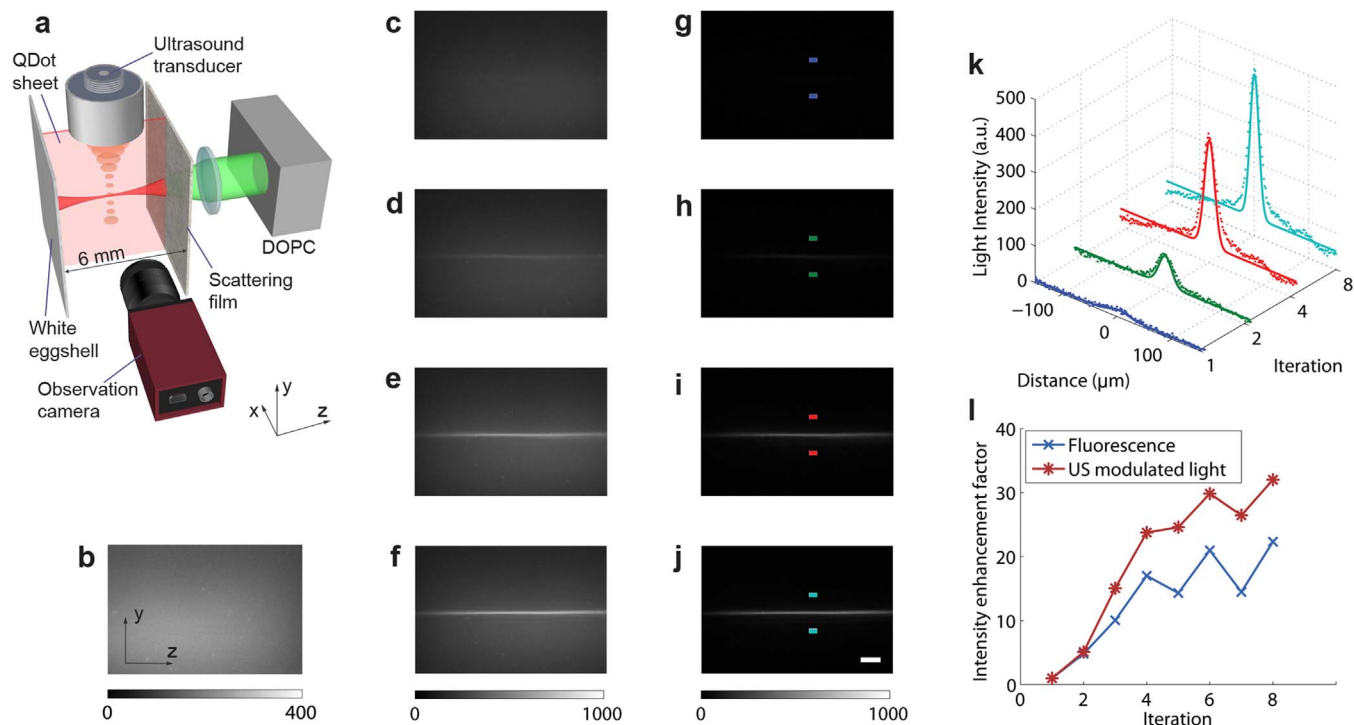
Figure 3 | Demonstration of intensity enhancement using iTRUE. (a) A 500 μm thick quantum dot sheet made of agarose was sandwiched between a layer of scattering film and a piece of white eggshell. The probe beam of the DOPC system entered the sample via the film side. An observation camera with a fluorescence filter was used to observe the cutaway view of the emission light from the quantum dot sheet. This camera imaged at the focus of the ultrasound, which was located in the centre of the quantum dot sheet. (b) The emission light without TRUE (the SLM was loaded with a random pattern). (c–f) Emission beam profiles with iTRUE iterations of 1, 2, 4 and 8 times, respectively. (g–j) Light beam profiles with background–subtraction. (k) One-dimensional images and the corresponding Gaussian fitting curves at the focus of the ultrasound (the area between the colour blocks of g–j). (l) The light intensity enhancement factor, measured based on the fluorescence intensity observed by the observation camera and the ultrasound-modulated light measured by the DOPC system. The scale bar is 200 μm.

reduce this effect, one solution would be to combine the measured phase map with the previous measured phase maps for iTRUE play-back at each iteration, rather than complete replacement of the phase map. However, the intensity optimisation process would be slower in this case.

Image scanning. To quantify the resolution improvement using our iTRUE system, we imaged a 15 μm fluorescent bead by raster scanning. The experimental setup was the same as that used for direct visualisation of the focal beam, except that the quantum dot sheet was replaced with a fluorescent bead and the observation camera was used as a single channel photodetector (Fig. 4a). Microscopic images of the fluorescent bead on a microscope slide without and with the scattering film are shown in Fig. 4b and c. It should be noted that the image shown in Fig. 4c was taken with scattering film attached to a piece of conventional microscope cover glass that covered the fluorescent bead. In the sample, the bead was placed 3 mm behind the scattering film. In order to scan the iTRUE focus across the fluorescent bead, the ultrasound transducer was moved in the x-y plane with a 10 μm step size and 11 steps in each direction (110 μm × 110 μm in total). At each step, 6 iterations were carried out. In order to compare the performance of conventional TRUE and iTRUE with different numbers of iterations, the SLM was loaded with a random pattern at the beginning of each scanning step. The fluorescent intensity was measured when the random pattern was displayed on the SLM (background) and during each iteration. Background subtraction and cubic inter-polation were applied to each intensity map. Fig. 4d–i show the scanned fluorescence images from the 1st iteration (conventional TRUE) to the 6th iteration with a global colour map. The image

resolution in the ultrasound axial direction (y) and the lateral direction (x) were quantified by a fitting Gaussian profile to the one-dimensional bead images in both directions, as shown in Fig. 4d and i. The FWHMs of these Gaussian profiles were used to define the image resolution here. The axial and lateral resolutions of the fluorescent bead images are shown in Fig. 4j and k, respectively. It can be observed that the axial resolution and lateral resolution were improved by ~2 times and ~3 times, respectively. The error bars shown in Fig. j and k indicate the 95% confidence bound of the curve fitting. Large error bars were observed at the first iteration because the light intensity was too low to provide a small fitting error.

Light focusing between biological samples. Focusing light in tissue in backscattering mode has a great potential in biological applications, where thick tissue or highly backscattering tissues like bone or are involved. Here, we investigated the light focusing capability of iTRUE in biological samples consisting of muscle tissue and cartilage. In order to directly visualise the focusing beam profile, a quantum dot sheet was also sandwiched between chicken muscle tissue (1 mm thick) and cartilage (Fig. 5a). By implementing iTRUE, the light intensity at the ultrasound focus increased progressively. The observation camera imaged the focusing beam profiles, as shown in Fig. 5b and c, in which images after the 1st iteration and the 16th iteration are compared. In order to measure the light intensity at the foci quantitatively, one dimensional images across the foci were taken using the same method as that used for Fig. 3k. It should be noted that two dimensional images at the 2nd, 4th and 8th iteration are not shown here. Gaussian functions were also fitted to these one dimensional images (Fig. 5d). By taking the ratio between the Gaussian profile amplitude of the 16th iteration and the
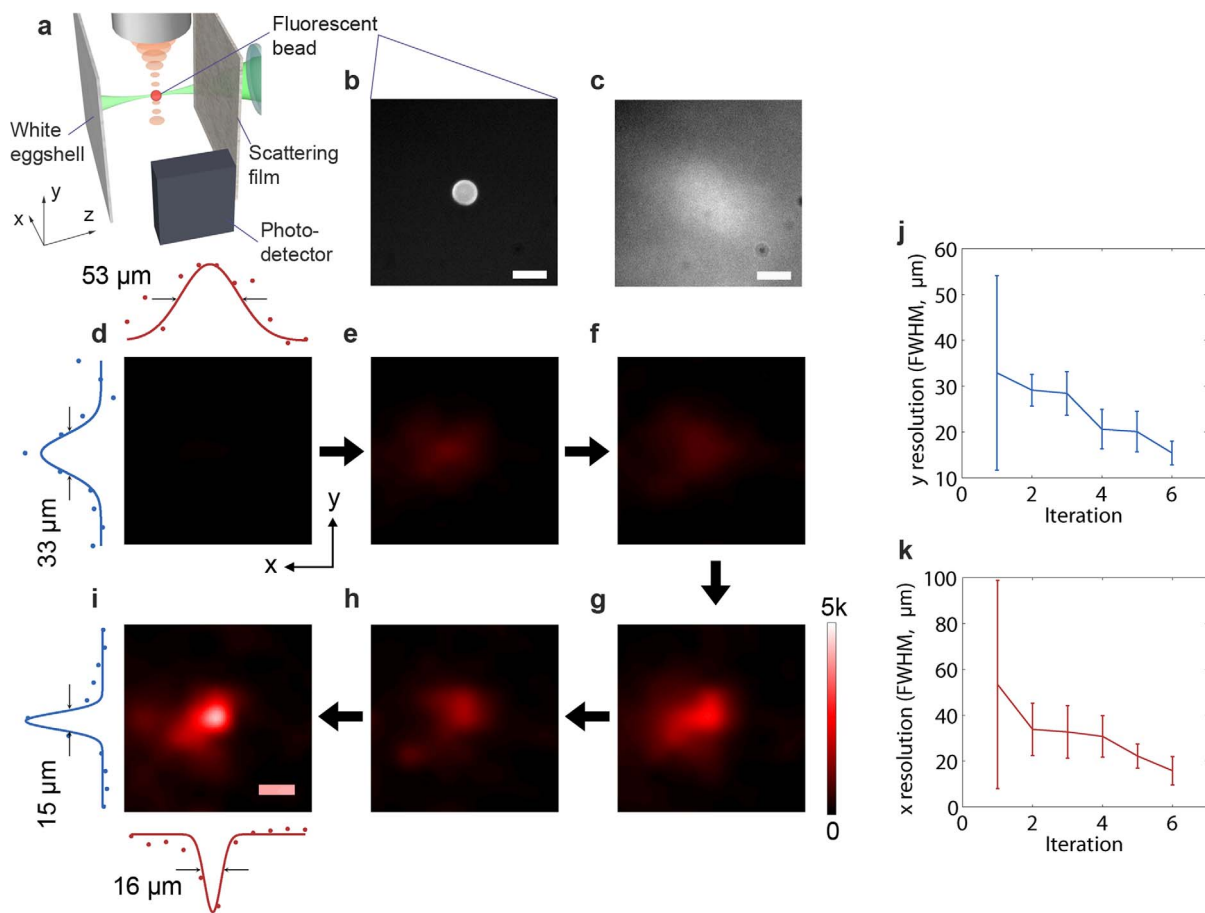
Figure 4 | Image scanning of a fluorescent bead. (a) Experimental setup. The ultrasound focus scanned the sample in the x-y plane. At each step, 6 iTRUE iterations were implemented. The fluorescence intensity was measured at each iteration using the photodetector. (b–c) Microscopic images of the fluorescent bead without and with the scattering film. (d–i) Intensity map of the fluorescent signals (11 × 11 scanning points with cubic interpolation). A Gaussian profile was fitted to the data points across the centre of the bead in both the x and y directions. (j, k) The resolution (FWHM of the Gaussian profile) in the y direction and the x direction of the fluorescent bead image over 6 iterations. The error bars indicate the 95% confidence bound. All scale bars are 20 μm.

1st iteration, an intensity enhancement factor of 18 was achieved. The light intensity was saturated after ~12 iterations, which is more than that required in the previous case with the scattering film and eggshell sample (~8 iterations). One reason for this difference is that the chicken muscle tissue scatters more light than the scattering film. Therefore, the initial ultrasound-encoded light intensity is lower and more iterations are required before saturation.

Discussion

The TRUE technique provides a non-invasive approach to focus light inside scattering media such as biological samples. This technique can be applied to a wide variety of applications such as deep tissue fluorescence imaging, photodynamic therapy, laser surgery and optogenetics. Some of the key factors making TRUE practical for these applications are its high focusing efficiency, higher resolution and the capability for backscattering mode operation. The proposed iTRUE technique provides an elegant solution for signal enhancement, resolution improvement and backscattering mode operation. The tissue-cartilage sample used in the experiment here mimics the structure that can be found in many parts of biological bodies. This is a significant step to move TRUE toward biological laboratories and clinics.

We explained the intensity enhancement mainly in the view of SNR throughout the principle section. However, there could be other mechanisms that also contribute to the intensity enhancement. One potential mechanism is the reduction of the optical mode at the

ultrasound focus because iTRUE reduces the size of the optical focus. In this case, the ratio between the number of controllable optical modes and the number of optical modes contained in the ultrasound focus increases[1,12]. The intensity of the background light also increases over iterations (Fig. 3c–f). This effect could attribute to the possibility that the light intensity tends to be redistributed on the transmission channels with a higher transmission coefficient during the iteration process[22]. The maximum achievable PBR with iTRUE is limited by the noise present on the measured phase map, the size of the ultrasound focus and the number of controllable optical modes. In practice, the PBR of iTRUE is also limited by the achievable PBR of the DOPC system and the profile of the ultrasound focus.

Resolution improvement with iTRUE has been demonstrated experimentally and theoretically. The resolution can be improved because the profile of the ultrasound focus can be approximated to be Gaussian. The photons tend to focus back to the strongest modulated optical mode, which gives the highest modulated signals. In practice, the ultrasound profile is very 'flat' compared to the size of an optical speckle. Therefore, the resolution improvement is limited. The resolution was improved less in the experiment than in the simulation, possibly because of the timing jitter between the ultrasound and laser pulses in our experiment.

Although only backscattering mode is demonstrated here, we expect it would not be difficult to implement the iTRUE system in transmission mode. One simple solution would be to place a mirror
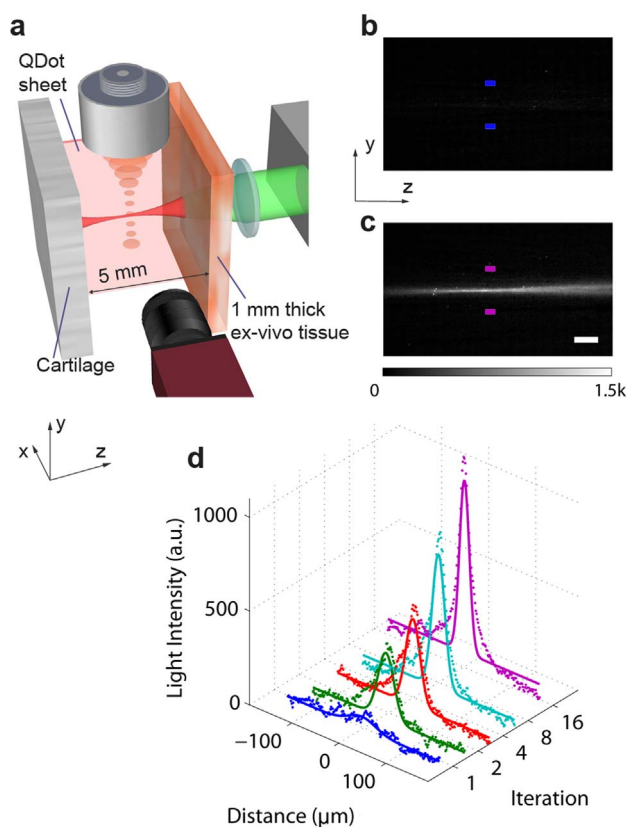
Figure 5 | Observation of light intensity enhancement in biological samples. (a) Sample setup. The sample consisted of a piece of chicken tissue (1 mm thick) and cartilage, with a quantum dot sheet sandwiched between them for visualisation purpose. (b–c) Image observed by the camera after the 1st iteration (b) and the 16th iteration (c) of iTRUE. (d) One dimensional images of the light foci after the 1st, 2nd, 4th, 8th and 16th iterations. These images were taken from the corresponding area between the two colour coded blocks shown in (b) and (c) (only the 1st and 16th images are shown). The scale bar is 200 μm.

on the other side of the sample when transmission mode is needed. In transmission mode, the sample is usually thin and most of the light is forward scattered. In this case, the mirror would effectively reflect the forward scattered light back to the camera. This approach is similar to the case of folding one of the DOPC setups along the mirror plane in a 2-DOPC TRUE system[19], but the key difference is the capability of simultaneous playback and recording in a single DOPC system.

Currently, the operation time of TRUE (for a single iteration of wavefront measurement and playback) is approximately 1 s. This limits its biomedical applications to *ex-vivo* tissue samples or immobilised living tissue due to optical speckle decorrelation[23]. The overall implementation time of iTRUE increases by a factor of the iteration number. However, iterations will not make the decorrelation problem worse than for the TRUE case because iTRUE updates the phase map during each iteration. The decorrelation problem is only limited by the duration of a single iTRUE iteration, which is the same as that of TRUE. Therefore, similar to TRUE, the timing issue can be further improved by reducing the averaging frames for the phase recording using an off-axis holography for phase measurement and a faster SLM. For biomedical imaging, the overall scanning speed of the current iTRUE technique limits its application to a low number of sampling points. However, the overall image scanning speed of iTRUE can be further improved by using a continuous scanning scheme[20]. Importantly, focusing light inside biological tissue is also useful for other applications, such as photodynamic therapy, laser

surgery and optogenetics, in which fewer scanning points are required.

Methods

Setup. The iTRUE system was custom-built, and the full system diagram is shown in the supplementary document. In our experiment, a 2.7 W, 532 nm wavelength Q-switch laser (Navigator, Spectra-Physics, USA) generated pulses with a 20 kHz repetition rate, a 7 ns pulse width and a 7 mm coherent length. The laser beam was split into a reference beam and probe beam. Both beams were spatially filtered by single mode fibres and collimated.

Ultrasound pulse trains were generated by a focused ultrasound transducer (50 MHz central bandwidth, 6.35 mm element diameter, 6 mm focal length; V3330, Olympus, USA), which provided a focal width of ∼30 μm (−6 dB). The ultrasound pulses were synchronised with the laser pulses, and a delay was added to make them coincide at the focus of the ultrasound transducer.

The collimated probe beam was coupled to an SLM (Pluto, Holoeye, Germany) by a 50/50 beam splitter. The reflected light from the SLM entered the sample through a 50 mm focal lens whose focus was located around the focal point of the transducer. The back scattered light from the sample was then reflected to a sCMOS camera (PCO.edge, PCO, Germany) by a 50/50 plate beam splitter (High-Energy Nd:YAG Laser, Newport Cooperation, USA). The camera plane and the SLM plane were virtually matched through this beam splitter. The reference beam was combined with the backscattered modulated light using a 90/10 transmission-reflection beam splitter, creating an interfering pattern on the camera.

Phase recording. A detailed signal flow diagram is shown in supplementary document. In order to selectively detect the ultrasound-modulated light using a camera, the frequency of the reference beam was shifted by 50.010 MHz using an acousto optic modulator (AFM-502-A1, IntraAction, USA). Consequently, the unmodulated light was washed out because the 20 kHz laser pulses cannot lock at this beating frequency (50.010 MHz). However, the ultrasound pulses from the transducer were inverted one after another so that the beating frequency between the ultrasound modulated light and the reference beam could be locked[24,25]. A 4-phase stepping digital holography method[21] was used to measure the phase of the ultrasound-modulated light. In this case, two clock sources were used in our system. The first was generated by a digital delay generator (DG645, Stanford Research Systems, USA), which generates a 20 kHz trigger signal for the laser and ultrasound. The pulse inversed ultrasound signal was generated by a function generator (AFG 3252, Tektronix, USA) and amplified by a RF power amplifier (30W1000B, Amplifier Research, USA). The reference beam signal was generated by another function generator of the same model, which was also synchronised with a digital delay generator. The other clock source was generated by a digital acquisition DAQ board (PCI6111, National Instruments, USA), which was used to synchronise the camera and the phase-shifting signal for digital hologram recording. This phase-shifting signal modulated the phase of the reference beam signal through the function generator by 0, π/2, π and 3π/2. Therefore, four interfering patterns (I_0, $I_{\pi/2}$, I_π and $I_{3\pi/2}$) were captured on the camera (28 ms exposure time, 25 frames/s, 5 frames for each phase for averaging purposes). The complex field can then be calculated as $E = (I_0-I_\pi) + i(I_{\pi/2}-I_{3\pi/2})$, where i denotes the imaginary part.

Alignment. A protocol[26] was previously developed for the alignment of a DOPC system, which is the core of the iTRUE system. The DOPC system used in iTRUE differs from the previous system in that a separated reference beam and playback beam are required for simultaneous playback and recording in the iTRUE system. This requirement poses a larger challenge in aligning the DOPC system because more variables are involved. Three major steps were implemented to align the DOPC system. First, the flatness between the SLM and the collimated probe beam was assured by searching for an optimised compensation phase map. This step minimised problems due to aberration of the collimated lens and unevenness of the SLM surface. In this case, the SLM pixels were scanned for the maximum light intensity through the single mode fibre, which spatially filtered the probe beam before collimation. Second, the camera plane and the SLM plane were roughly aligned such that a discernable DOPC focus could be obtained through a thin scattering medium. Third, a digital wave propagation method was used to tune the virtual position of the camera or the SLM subject to the maximum light intensity of the DOPC focus.

Simulation. The simulation was based on a shot noise limited model. Starting with the initial probe beam, whose phase was uniformly distributed over 0–2π, the scattered light field inside a scattering medium can be obtained by multiplying the probe beam vector with a transmission matrix. An ultrasound profile with a Gaussian function shape was used to modulate the scattered field vector by scalar multiplication. The width of this Gaussian function was such chosen that the ratio between the number of controllable modes and the number of modes within the ultrasound focus was ∼100, which is a typical number in TRUE[12]. The ultrasound modulated field was then propagated back through the scattering medium by multiplying the transpose of the transmission matrix. The resulting field was added to shot noise with a Poisson distribution, resulting in phase error. The phase of the conjugated field was used to imprint a blank probe beam, which is the starting point of another iteration loop. Assuming that the recorded field is measured by 4-phase stepping digital holography, the SNR of the recorded interferogram, the phase error of

6

the recorded field and the light intensity at the ultrasound focus can be simulated and recorded during each iteration loop.

Sample preparation. To make a quantum dot sample, quantum dots (Qtracker 655 non-targeted quantum dots, Invitrogen) were mixed with a 1.5% agarose gel in the aqueous phase. The mixture was cast in a 500 μm thick mould and transferred to a glass cuvette. The empty space in the glass cuvette was filled with clear agarose gel of the same concentration.

To make a fluorescence bead sample, a 15 μm fluorescent bead (FluoSpheres 580/605 polystyrene microsphere, Invitrogen) was placed on top of a block of agarose gel in the solid phase. After verifying placement with a fluorescence microscope, the fluorescent bead was secured with extra agarose gel of the same concentration.

The cartilage was excised from the joint of a fresh chicken leg. The size of the cartilage was 10 mm (x) × 5 mm (y) × 2 mm (z) in the coordinates shown in Fig. 5a. The muscle tissue was excised from a piece of chicken breast. The size of the tissue was approximately 10 mm (x) × 5 mm (y) × 1 mm (z) in the same coordinate system.

1. Vellekoop, I. M. & Mosk, A. P. Focusing coherent light through opaque strongly scattering media. *Opt. Lett.* **32**, 2309–2311 (2007).
2. Popoff, S. M. *et al.* Measuring the Transmission Matrix in Optics: An Approach to the Study and Control of Light Propagation in Disordered Media. *Phys. Rev. Lett.* **104**, 100601 (2010).
3. Yariv, A. Phase conjugate optics and real-time holography. *Quantum Electron. IEEE J.* **14**, 650–660 (1978).
4. Yaqoob, Z., Psaltis, D., Feld, M. S. & Yang, C. Optical phase conjugation for turbidity suppression in biological samples. *Nat Phot.* **2**, 110–115 (2008).
5. Cui, M. & Yang, C. Implementation of a digital optical phase conjugation system and its application to study the robustness of turbidity suppression by phase conjugation. *Opt. Express* **18**, 3444–3455 (2010).
6. Vellekoop, I. M. & Aegerter, C. M. Scattered light fluorescence microscopy: imaging through turbid layers. *Opt. Lett.* **35**, 1245–1247 (2010).
7. Jang, M., Sentenac, A. & Yang, C. Optical phase conjugation (OPC)-assisted isotropic focusing. *Opt. Express* **21**, 8781 (2013).
8. Conkey, D. B., Caravaca-Aguirre, A. M. & Piestun, R. High-speed scattering medium characterization with application to focusing light through turbid media. *Opt Express* **20**, 1733–1740 (2012).
9. Chaigne, T. *et al.* Controlling light in scattering media non-invasively using the photoacoustic transmission matrix. *Nat. Photonics* **8**, 58–64 (2013).
10. Hsieh, C., Pu, Y., Grange, R. & Psaltis, D. Digital phase conjugation of second harmonic radiation emitted by nanoparticles in turbid media. *Opt. Express* **18**, 533–537 (2010).
11. Xu, X., Liu, H. & Wang, L. V. Time-reversed ultrasonically encoded optical focusing into scattering media. *Nat Phot.* **5**, 154–157 (2011).
12. Wang, Y. M., Judkewitz, B., DiMarzio, C. A. & Yang, C. Deep-tissue focal fluorescence imaging with digitally time-reversed ultrasound-encoded light. *Nat Commun* **3**, 928 (2012).
13. Si, K., Fiolka, R. & Cui, M. Fluorescence imaging beyond the ballistic regime by ultrasound pulse guided digital phase conjugation. *Nat. Photonics* **6**, 657–661 (2012).
14. Tay, J. W., Lai, P., Suzuki, Y. & Wang, L. V. Ultrasonically encoded wavefront shaping for focusing into random media. *Sci. Rep.* **4**, 3918 (2014).
15. Suzuki, Y. Energy enhancement in time-reversed ultrasonically encoded optical focusing using a photorefractive polymer. *J. Biomed. Opt.* **17**, 080507 (2012).
16. Judkewitz, B., Wang, Y. M., Horstmeyer, R., Mathy, A. & Yang, C. Speckle-scale focusing in the diffusive regime with time reversal of variance-encoded light (TROVE). *Nat Phot.* **7**, 300–305 (2013).
17. Jang, M., Ruan, H., Judkewitz, B. & Yang, C. Model for estimating the penetration depth limit of the time-reversed ultrasonically encoded optical focusing technique. *Opt Express* **22**, 5787–5807 (2014).
18. Lai, P., Xu, X., Liu, H., Suzuki, Y. & Wang, L. V. Reflection-mode time-reversed ultrasonically encoded optical focusing into turbid media. *J. Biomed. Opt.* **16**, 080505 (2011).
19. Si, K., Fiolka, R. & Cui, M. Breaking the spatial resolution barrier via iterative sound-light interaction in deep tissue microscopy. *Sci. Rep.* **2**, 748 (2012).
20. Suzuki, Y., Tay, J. W., Yang, Q. & Wang, L. V. Continuous scanning of a time-reversed ultrasonically encoded optical focus by reflection-mode digital phase conjugation. *Opt. Lett.* **39**, 3441–4 (2014).
21. Yamaguchi, I., Matsumura, T. & Kato, J.-I. Phase-shifting color digital holography. *Opt. Lett.* **27**, 1108–10 (2002).
22. Vellekoop, I. M. & Mosk, A. P. Universal optimal transmission of light through disordered materials. *Phys. Rev. Lett.* **101** (2008).
23. Cui, M., McDowell, E. J. & Yang, C. An in vivo study of turbidity suppression by optical phase conjugation (TSOPC) on rabbit ear. *Opt. Express* **18**, 25–30 (2010).
24. Ruan, H., Mather, M. L. & Morgan, S. P. Pulsed ultrasound modulated optical tomography with harmonic lock-in holography detection. *J. Opt. Soc. Am. A. Opt. Image Sci. Vis.* **30**, 1409–16 (2013).
25. Ruan, H., Mather, M. L. & Morgan, S. P. Pulsed ultrasound modulated optical tomography utilizing the harmonic response of lock-in detection. *Appl. Opt.* **52**, 4755–62 (2013).
26. Jang, M., Ruan, H., Zhou, H., Judkewitz, B. & Yang, C. Method for auto-alignment of digital optical phase conjugation systems based on digital propagation. *Opt. Express* **22**, 14054 (2014).

Acknowledgments

Author contribution

H.R., M.J., B.J. and C.Y. conceived the idea. H.R., M.J. and B.J. designed the experiment. H.R. and M.J. carried out the experiment and data analysis. The simulation was carried out by H.R. All authors contributed to the preparation of the manuscript.

Additional information